

# Thermorheological Behavior of Polypropylene and Polycarbonate Inclusions in an Ethylene Copolymer Matrix

V. NASSIET,<sup>1</sup> P. CASSAGNAU,<sup>2</sup> A. ALLAL,<sup>1</sup> J. P. MONTFORT<sup>1</sup>

<sup>1</sup> Laboratoire de Physique des Matériaux Industriels, ESA—CNRS 5067, Université de Pau et des Pays de l'Adour, 64000 Pau, France

<sup>2</sup> Laboratoire des Matériaux Organiques à Propriétés Spécifiques, CNRS, Verraison, France

Received 12 February 1997; accepted 27 March 1997

**ABSTRACT:** We investigated the rheological behavior of incompatible polymer blends made of a semicrystalline ethylene–methyl acrylate (EMA) matrix and two different species of inclusions—a semicrystalline polypropylene and an amorphous polycarbonate. The emulsion model of Palierne which describes the linear viscoelastic behavior of incompatible blends of polymers was applied to both polymer blends at temperatures below and above the melt or glass temperature of the dispersed polymer. The Palierne model fits well the experimental results for temperatures above the transition temperatures of the minor phases. When the dispersed phase is rigid, the fit is good all over the frequency range for the blend of EMA/polypropylene (PP), whereas a noticeable deviation occurs at low frequencies for the EMA/polycarbonate (PC). That behavior is explained by strong van der Waals interactions between EMA and PC molecules, which creates a layer of EMA chains irreversibly adsorbed onto the PC surface. © 1997 John Wiley & Sons, Inc. *J Appl Polym Sci* **66**: 179–186, 1997

**Key words:** viscoelasticity; polymer blend; Palierne's model; van der Waals interaction; adsorption

## INTRODUCTION

Mechanical measurements are known to be very useful for the characterization of incompatible polymer blends. The linear viscoelastic behavior of incompatible blends of polymers can be interpreted in terms of emulsion models. The main feature is the presence of a relaxation domain which appears in the low-frequency zone. The most general emulsion model proposed by Palierne<sup>1</sup> explains this occurrence by the shape relaxation of the viscoelastic dispersed phase. Moreover, Palierne's theory encompasses previous

models dealing with either incompressible elastic materials<sup>2</sup> or elastic spheres dispersed in a Newtonian matrix<sup>3</sup> or blends of viscous and viscoelastic fluids.<sup>4</sup> Therefore, it can be applied to polymer blends at temperatures below and above the melt or glass temperature of the dispersed polymer.<sup>5</sup> We are going to study the thermorheological behavior of incompatible polymer blends made of a semicrystalline ethylene–methyl acrylate (EMA) matrix and two different species of inclusions: a semicrystalline polypropylene and an amorphous polycarbonate (Table I). Due to the different transition temperatures of the components, such systems can be used to check the changes occurring in the viscoelastic behavior at the transition temperature of the dispersed phase.

We expect that, at  $T > 160^{\circ}\text{C}$ , the phases are

---

Correspondence to: J. P. Montfort.

*Journal of Applied Polymer Science*, Vol. 66, 179–186 (1997)  
© 1997 John Wiley & Sons, Inc. CCC 0021-8995/97/010179-08

**Table I Transition Temperatures of the Pure Components**

Components	Glass Temperature (°C)	Melt Temperature (°C)
EMA	-30	50
PP	-30	160
PC	150	

behaving like viscoelastic liquids, and at  $50^\circ\text{C} < T < 150^\circ\text{C}$ , the spherical inclusions are rigid and the matrix remains viscoelastic. Therefore, we are going to check if the Palierne model applies in both cases.

## THEORY

For a binary mixture of viscoelastic materials without interparticle interactions, Palierne<sup>1</sup> expressed the complex shear modulus  $G^*(\omega)$  as the function of the individual complex shear moduli— $G_M^*$  for the matrix and  $G_I^*$  for the dispersed phase—of the volume fraction  $\phi_i$  of droplets with a radius  $R_i$  and of the interfacial tension  $\alpha$ . A distribution of size and composition of the dispersed phase is taken into account. The expression of  $G^*(\omega)$  is

$$G^* = G_M^* \frac{1 + 3 \sum_i \phi_i H_i}{1 - 2 \sum_i \phi_i H_i} \quad (1)$$

with

$$H_i = \frac{(4\alpha/R_i)(2G_M^* + 5G_I^*) + (G_I^* - G_M^*)(16G_M^* + 19G_I^*)}{(40\alpha/R_i)(G_M^* + G_I^*) + (2G_I^* + 3G_M^*)(16G_M^* + 19G_I^*)} \quad (2)$$

The summation is carried out over the distribution of droplet sizes. For a narrow distribution of particle sizes, a good agreement is obtained between the model predictions and the experimental data if the summation over the distribution of particle sizes and of volume fractions are, respectively, replaced by the volume-average particle radius  $R$  and the total volume fraction of the dispersed phase  $\phi$ .<sup>6</sup> In that case, eq. (1) is treated without any polydispersity effect, assuming that

$$\sum_i \phi_i H_i(R_i) = \phi H(R) \quad (3)$$

Palierne's model can be used for a blend of two viscoelastic phases when the behavior of each component and the interfacial tension are known. When the interfacial tension is unknown, the model is a means to determine that value by fitting theoretical curves to experimental data. In the above form, Palierne's model can be applied at  $T > 160^\circ\text{C}$  when the components of the EMA/polypropylene (PP) and EMA/polycarbonate (PC) blends are viscoelastic liquids.

When applying the above expression to suspensions where the dispersed phase is made of rigid and elastic spheres—the case of EMA/PP and EMA/PC blends studied at  $80^\circ\text{C} < T < 150^\circ\text{C}$ — $G_I^*$  reduces to an elastic modulus which is much higher than is the modulus of the matrix. Therefore, eq. (1) is replaced by

$$G^* = G_M^* \frac{1 + \frac{3}{2} \sum_i \phi_i}{1 - \sum_i \phi_i} \quad (4)$$

where the complex shear modulus of the blend is just proportional to that of the matrix by a factor

$$b(\phi) = \frac{1 + \frac{3}{2} \sum_i \phi_i}{1 - \sum_i \phi_i}$$

## EXPERIMENT

### Materials

The polypropylene (PP) and the EMA copolymer containing in weight 29% of methyl acrylate were synthesized by Atochem. The polycarbonate (PC) used was a commercial product synthesized by Bayer. The respective molecular weights obtained by GPC are as follows: EMA:  $M_w = 94,300$  g/mol and  $M_n = 22,000$  g/mol; PP:  $M_w = 74,920$  g/mol and  $M_n = 19,440$  g/mol; and PC:  $M_w = 37,585$  g/mol and  $M_n = 19,226$  g/mol.

The EMA/PP and the EMA/PC blends were mixed in a twin-screw extruder from Leistritz (LSM30-34). The volume fractions of PP and PC in the EMA matrix were equal to 0.10. The mixtures were compression-molded at  $180^\circ\text{C}$  and 3 bars for 10 min.

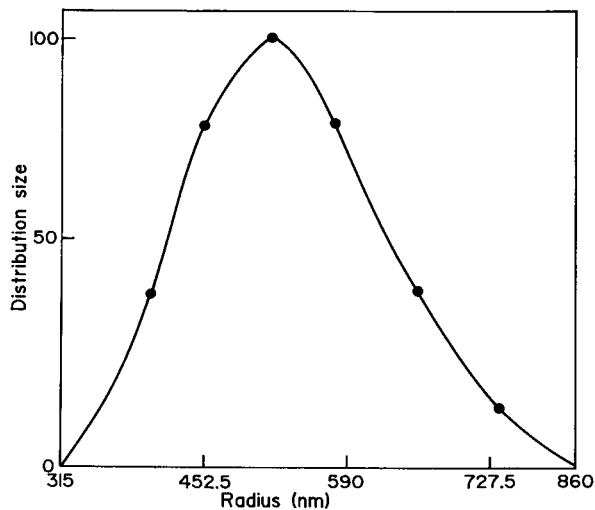


**Figure 1** Distribution size of the PP spherical inclusions in the EMA matrix vs. the radius.

### Morphological Analysis

Dynamic light scattering was performed to determine the particle-size distribution of PP particles. Experimentally, the EMA/PP blend was dissolved in tetrahydrofuran (THF). At room temperature, THF is only a good solvent of the EMA phase. Then, the inclusions of PP remain in a solid state and behave as a suspension of particles with the size distribution of the blend. Figure 1 shows the particle-size distribution of the blend from which the weight- and number-average diameters, respectively,  $R_v$  and  $R_n$ , can be calculated:  $R_v = 541$  nm and  $R_n = 527$  nm. The EMA/PC morphology was examined by scanning electron microscopy. The contrast between PC and EMA is weak. Nevertheless, PC inclusions can be discerned in Figure 2 and their average diameter is close to  $1 \mu\text{m}$ . Since the polydispersity is very narrow for both blends, the particle-size distribution is negligible and eq. (1) is used without any polydispersity effect.

### Rheological Tests

The rheological behavior of PC, PP, and EMA and of the blends was investigated by using a stress-imposed rheometer (Rheometrics D.S.R.). From oscillatory experiments, one deduces the complex compliance  $J^*(\omega)$ , which is the reciprocal of the complex shear modulus  $G^*(\omega)$ , within a frequency range of about  $10^{-4}$  to  $10^3 \text{ s}^{-1}$ . With that technology, values as low as  $10^{-3}$  Pa can be obtained with an accuracy of 5%. Furthermore, with

the equipment that we used, it is possible to change the temperature from room temperature to  $350^\circ\text{C}$ . That can lead to an extension of the width of the relaxation spectrum when the time-temperature superposition principle holds.

Small-amplitude oscillatory shear measurements were carried out with a parallel-plate geometry (diameter of the plates: 25 mm). Prior to testing, the samples were dried under a vacuum for 2 days at  $90^\circ\text{C}$  for PP and PC and at room temperature for EMA and for the two blends. The experiments were done under a continuous purge of dry nitrogen. No thermal degradation occurred during the measurements as checked by repeated measurements and by comparison with the initial data. Moreover, we verified the stress-strain linearity for all experiments.

## RESULTS AND DISCUSSION

The experimental temperature range was  $110$ – $200^\circ\text{C}$  for all samples. Master curves for  $G'$  and  $G''$  as a function of the frequency were drawn at two reference temperatures  $T_r$ , using the time-temperature superposition principle:  $T_r = 140^\circ\text{C}$  for the data between  $110$  and  $140^\circ\text{C}$  and  $T_r = 200^\circ\text{C}$  for the data between  $160$  and  $200^\circ\text{C}$ .

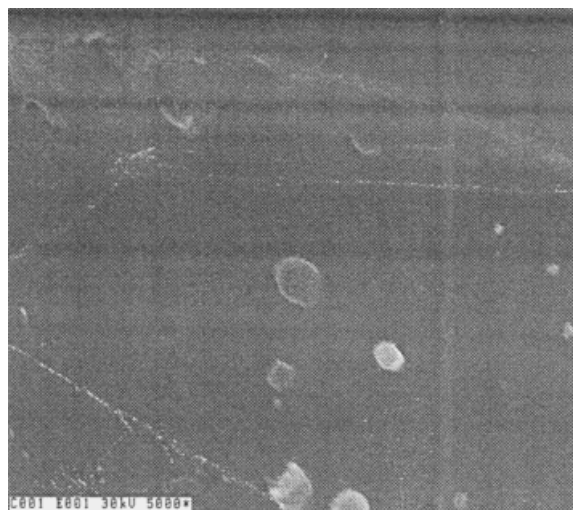


**Figure 2** Photograph of the EMA/PC blend. The contrast is poor and does not allow one to determine a size distribution.

**Table II Temperature Shift Factors of the Matrix and the Blends with Two Reference Temperatures  $T_r$ : (a)  $T_r = 200^\circ\text{C}$ ; (b)  $T_r = 140^\circ\text{C}$**

$T$ ( $^\circ\text{C}$ )	EMA	EMA/PC	EMA/PP
(a)			
160	6.3	6.35	5.5
170	2.6	2.2	2.3
180	1.4	1.44	1.2
200	1	1	1
(b)			
110	4.5	5	4.8
120	3.3	3.55	3.45
130	2	1.37	1.36
140	1	1	1

The thermal shift factors  $a_T$  are listed in Table II(a) and (b) for the matrix and the two blends. They are very close to one another because of the low concentration of the dispersed phase. The  $G'$  and  $G''$  master curves of the components are shown in Figure 3 and their rheological parameters in the terminal zone, at  $T = 200^\circ\text{C}$ , are given in Table III.

The terminal relaxation time is defined as the reciprocal of the frequency corresponding to the maximum of the imaginary part  $\eta''$  of the complex viscosity  $\eta^*$  in a Cole and Cole plot.

The viscosity ratio  $k = \eta_I/\eta_M$  ( $I$ : inclusions;  $M$ :

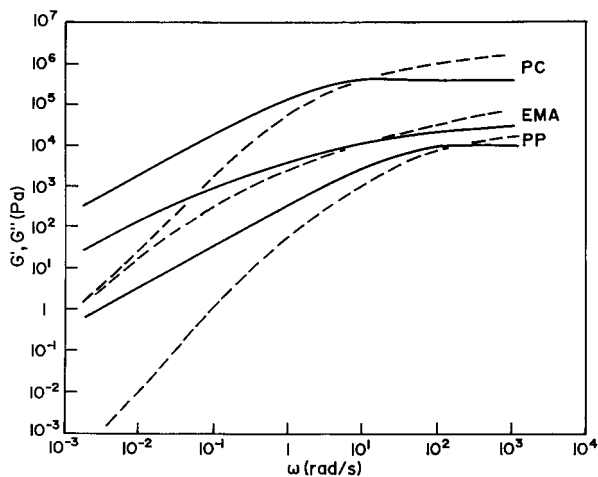


**Figure 3** Variation of (---) the elastic modulus ( $G'$ ) and (—) the loss modulus ( $G''$ ) for PP, PC, and EMA. The reference temperature  $T_r$  is  $200^\circ\text{C}$ . The master curves are drawn in the frequency range covered by the stress-imposed rheometer.

**Table III Viscoelastic Parameters of the Pure Components at  $200^\circ\text{C}$**

Sample	Zero-shear Viscosity (Pa-s)	Terminal Relaxation Time (s)
EMA	19,000	20
PC	220,000	0.8
PP	300	0.5

matrix) equals 0.075 for the EMA/PP blend and 27.5 for the EMA/PC blend. The relaxation time ratio  $\chi = \lambda_I/\lambda_M$  equals 0.0125 for the EMA/PP blend and 0.025 for the EMA/PC blend. Moreover, we can notice that the usual frequency dependence in the terminal zone—i.e.,  $G' \propto \omega^2$  and  $G'' \propto \omega$ —is shifted toward inaccessible low frequencies because of the high matrix polydispersity. That is the reason why we used a Cole and Cole plot of the viscosities to evaluate the zero shear viscosity and an average terminal relaxation time.

Figures 4 and 5 show that the rheological behaviors of the blends at  $200^\circ\text{C}$  are intermediate between the rheological behavior of the components and close to that of the matrix. The Palierne expression [eq. (1)] fits very well the experimental results when taking for  $G_I^*(\omega)$  and  $G_M^*(\omega)$  the experimental data of the pure components, and for the interfacial tension  $\alpha$ , the values calculated from the surface tensions of the components.<sup>7</sup>

The surface tension  $\gamma$  is related to its components by

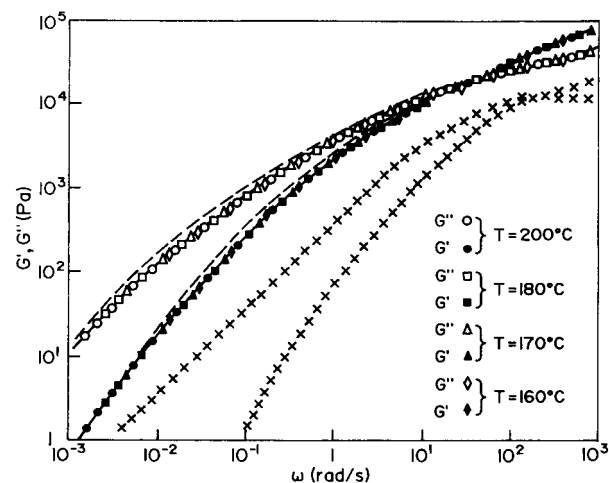


**Figure 4** Master curves of the complex shear modulus of EMA/PP blend and of the pure components: ( $\times$ ) PP; (---) EMA.  $T_r = 200^\circ\text{C}$ . (—) Comparison with eq. (1).

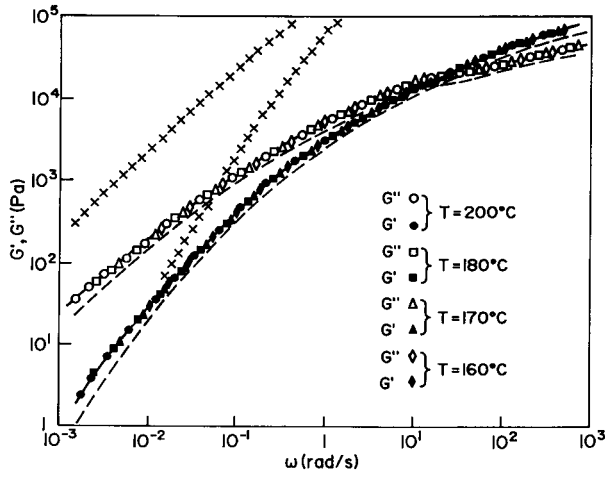


**Figure 5** Master curves of the complex shear modulus of EMA/PC blend and of the pure components: (×) PC; (—) EMA.  $T_r = 200^\circ\text{C}$ . (—) Comparison with eq. (1).

$$\gamma = \gamma^d + \gamma^p \quad (5)$$

where  $\gamma^d$  and  $\gamma^p$  are, respectively, the dispersive component and the polar component. The values of  $\gamma^d$  and  $\gamma^p$  for the polymers are calculated from the contact angles with two reference liquids (subscript  $i$ ) by using the harmonic-mean equation<sup>8</sup>:

$$(1 + \cos \theta_i) \gamma_i = 4 \left( \frac{\gamma_i^d \gamma_s^d}{\gamma_i^d + \gamma_s^d} + \frac{\gamma_i^p \gamma_s^p}{\gamma_i^p + \gamma_s^p} \right) \quad (6)$$

Diiodomethane and formamide are the two testing liquids for PC and PP. Ethylene glycol and  $\alpha$ -bromonaphtalene are the two testing liquids for EMA. The experimental values of the surface tension of the solid polymers are given in Table IV. Then, the interfacial tension  $\alpha$  between two polymers  $a$  and  $b$  is calculated from

$$\alpha = \gamma_a + \gamma_b - 4 \left( \frac{\gamma_a^d \gamma_b^d}{\gamma_a^d + \gamma_b^d} + \frac{\gamma_a^p \gamma_b^p}{\gamma_a^p + \gamma_b^p} \right) \quad (7)$$

For the EMA/PC blend, the calculated interfacial tension is  $\alpha_1 = 2.5 \pm 0.3$  mN/m, and for the EMA/PP blend,  $\alpha_2 = 1 \pm 0.1$  mN/m.

From the literature data of surface tensions, the variation of the interfacial tension with temperature<sup>9</sup> is given by

$$-\frac{d\gamma}{dt} = \frac{11}{9} \frac{\gamma_0}{T_c} \left( 1 - \frac{T}{T_c} \right)^{2/9} \quad (8)$$

where  $\gamma_0$  is the surface tension for  $T = 0$  K and  $T_c$  is the critical temperature. According to eq. (8), the surface tension is nearly constant at temperatures far below the  $T_c$ . Since the critical temperature of a polymer is typically  $600\text{--}900^\circ\text{C}$ , its surface tension is nearly constant within the experimental temperature range. That leads to a constant interfacial tension  $\alpha$ . When the two components are behaving as viscoelastic liquids, an additional relaxation domain is expected at low frequencies. According to Palierne, it is due to the shape relaxation of the spherical inclusions. The characteristic relaxation time and the amplitude of the domain are essentially functions of the viscosity ratio  $k$  and of the relaxation time ratio  $\chi$  of the two components. Graebing et al.<sup>10</sup> showed that a strong overlap of the domains occurs when the relaxation time ratio is lower than  $10^{-2}$ , which is the case of our experiments (Table III). Moreover, the fairly broad molecular weight distribution of the samples induces a broad distribution of the terminal relaxation times which favors the overlap of the two relaxation domains. Therefore, we cannot observe any noticeable signature of the shape relaxation of the viscoelastic particles.

At the reference temperature  $T = 140^\circ\text{C}$ , the PC and the PP inclusions are rigid, whereas the EMA matrix flows.  $G'$  and  $G''$  plots are shown in Figures 6 and 7 for both blends and the matrix. The main observation is that the complex shear modulus of the blends is proportional to that of the matrix, in agreement with eq. (4). However, if the fit is good all over the frequency range for the EMA–PP blend (Fig. 6), a noticeable deviation occurs at low frequencies for the EMA–PC blend (Fig. 7). As the inclusions are rigid, Palierne's model cannot predict an additional relaxation domain at low frequencies for the EMA/PC blend.

Slow relaxation processes have been detected experimentally for narrow polybutadiene samples filled with rigid silica spheres.<sup>11</sup> As in the case of

**Table IV** Dispersive and Polar Components of the Surface Tension of the Pure Polymers, Calculated by a Contact Angle Method

Samples	$\gamma^d$ (mN/m)	$\gamma^p$ (mN/m)	$\gamma = \gamma^p + \gamma^d$ (mN/m)
EMA	$35 \pm 2$	$1.1 \pm 0.05$	$36.1 \pm 3.5$
PC	$40 \pm 2$	$4.9 \pm 0.3$	$44.9 \pm 4.5$
PP	$29.1 \pm 1.5$	$0.50 \pm 0.05$	$29.6 \pm 3$

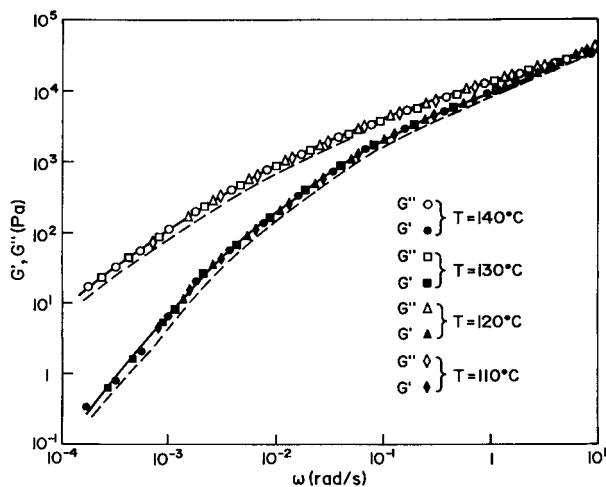


**Figure 6** (---) Master curves of the complex shear modulus of EMA/PP blend and of the EMA.  $T_r = 140^\circ\text{C}$ . (—) Comparison with eq. (4).

rigid PC inclusions, those secondary relaxation domains cannot be assumed due to a shape relaxation. They have been interpreted by a reversible adsorption of polybutadiene chains onto the silica surface which creates a monomolecular layer of the polymer. Its thickness is comparable to the bulk radius of gyration of the chains and its average relaxation time scales in the same way as do branches of star polymers. That picture has enabled us to modelize the additional relaxation domain at low frequencies by modifying the Palierne model.

The case of incompatible polymer blends is that of two low-energy materials with a weak revers-

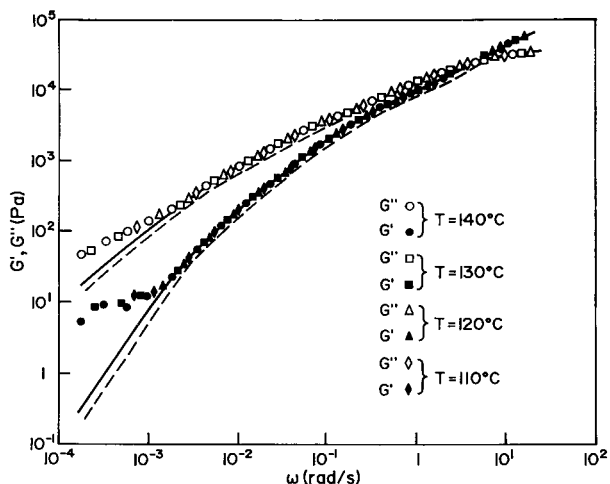


**Figure 7** (---) Master curves of the complex shear modulus of EMA/PC blend and of the matrix EMA.  $T_r = 140^\circ\text{C}$ . (—) Comparison with eq. (4).

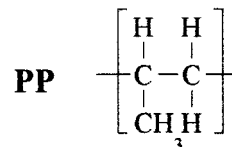
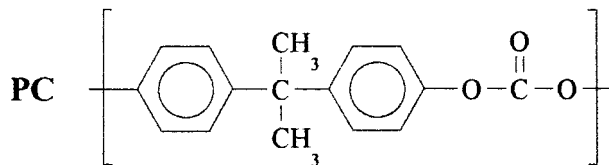
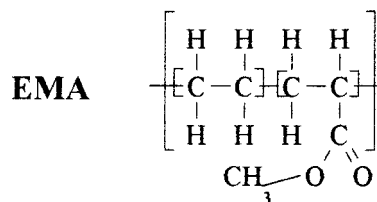


**Figure 8** Chemical formula of PP, PC, and EMA monomers.

ible adsorption. On the other hand, irreversible adsorption can exist between two molecules due to strong van der Waals interactions. Therefore, we can explain the different behavior of the EMA/PP and EMA/PC blends by the difference in the intensity of the molecular interactions. As there is no chemical reaction between the above components—no covalent or ionic bounds—the intermolecular forces can come from van der Waals forces or hydrogen bonding. The PP and EMA molecules do not interact strongly (Fig. 8) because the methyl groups are neutral for any other chemical entity. The van der Waals energy is about 1–1.5 kT. Then, the blend is thermorheologically identical to a suspension whose rheological behavior is predictable by eq. (4).

On the other hand, with the esterification being an equilibrium reaction, free hydroxyl groups can be present and generate hydrogen-bonded groups in the EMA/PC blend. On a Fourier transform infrared spectrum, the hydroxyl functions stretch between 3500 and 3000  $\text{cm}^{-1}$ . No band appears in the hydroxyl stretching region (Fig. 9). We can conclude that there is no hydrogen-bonding inter-

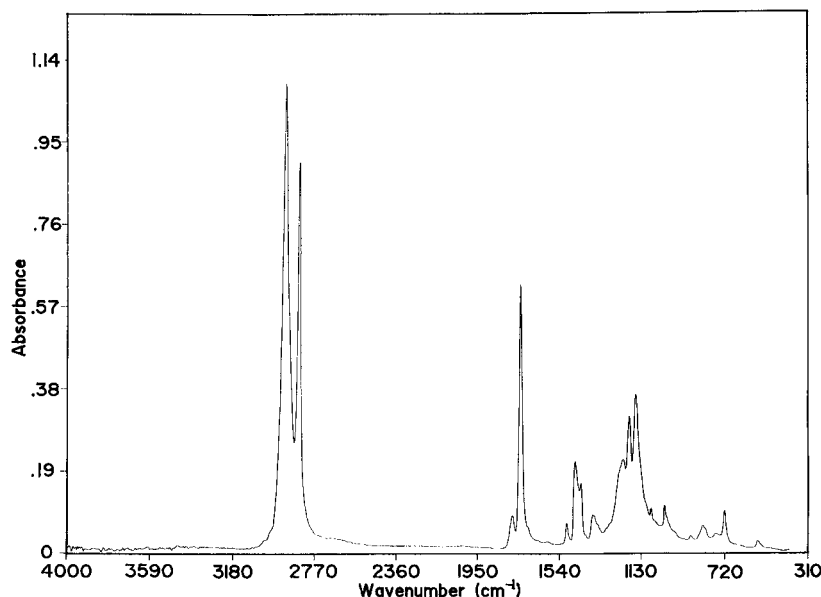


**Figure 9** Fourier transform infrared spectrum of the EMA/PC blend. There is no evidence of hydrogen bonds between the two polymers.

action in the EMA/PC blend. Nevertheless, PC inclusions and EMA molecules are strongly linked by their respective ester groups (Fig. 8). The permanent polarity of ester groups is responsible for a polar interaction (Keesom force) with an intensity of about 10 kT and that can explain the occurrence of a second relaxation domain. The very different values of  $\gamma^p$  for PP and PC strongly support that hypothesis. Therefore, we assume that EMA chains are irreversibly adsorbed on the PC surface. The methyl acrylate groups act as trains of the adsorbed chains and the ethylene sequences give rise to the loops and the tails of the adsorbed chains (Fig. 10). A quantitative analysis equivalent to that conducted with suspensions of silica spheres<sup>11</sup> requires a complete description of the additional relaxation domain and the knowledge

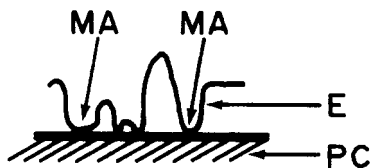


**Figure 10** Sketch of EMA chains adsorbed onto a rigid PC surface. The methyl acrylate sequences form trains and the ethylene sequences extend away from the surface. Their dynamics can be compared to that of the branches of a star polymer which diffuse in an environment made of other loops and of free EMA chains.

of the dynamics of the loops and the tails. Further experiments should be performed at much lower frequencies with well-defined statistical EMA chains. Furthermore, the dynamics of ethylene loops in a local environment of other ethylene sequences and of free EMA chains is not obvious to describe. At temperatures higher than the glass temperature of PC, we do not observe any deviation in the low-frequency region (Fig. 5), which is due to the fact that in that temperature range PC behaves as a liquid and the mobility of the carboxylic groups leads to a diffusion of the EMA chains in contact with the viscoelastic particles. Their relaxation time is close to that of the bulk EMA chains.

## CONCLUSION

We have tempted to show that if incompatible blends exhibit a rheological behavior dominated by that of the matrix, slow relaxation processes can appear and reveal two different mechanisms. At temperatures higher than the glass or melt temperature of the dispersed phase, the shape relaxation of the viscoelastic particles is responsible for an additional relaxation domain. Its contribution can be dominated by the diffusion process of the chains of the matrix when it is much slower than that of the chains of the dispersed polymer

( $\chi \ll 1$ ). Therefore, no evident signature of the shape relaxation of the particles can appear in the viscoelastic spectrum. At temperatures lower than the transition temperature of the dispersed species, the rheology of suspensions of rigid polymers in a viscoelastic matrix allows one to detect the presence of specific interactions between the two polymers. The formalism developed by Palierne holds when both components are viscoelastic. We have modified it<sup>11</sup> in order to take into account the specific dynamics of an interphase. That has been done for chains adsorbed at the surface of silica spheres and can be extended to incompatible blends. A quantitative study needs to work with well-defined samples. Furthermore, an interesting challenge is to conceive systems where a competition can occur between the shape relaxation of the inclusions and the dynamics of an interphase. Finally, it is worth noting that Palierne's analysis leaves aside the interparticle interactions which arise at high concentrations of the dispersed

phase. Such connectivity can be the cause of other relaxation processes.

## REFERENCES

1. J. F. Palierne, *Rheol. Acta*, **30**, 497 (1991).
2. E. H. Kerner, *Proc. Phys. Soc.*, **69**, 808 (1956).
3. H. Fröhlich and Sack, *Proceed. R. Soc. (Lond.)*, A, **185**, 415 (1946).
4. J. G. Oldroyd, *Proceed. R. Soc. (Lond.)* A, **218**, 122 (1953).
5. P. Cassagnau, *J. Appl. Polym. Sci.*, **58**, 1393–1399 (1995).
6. M. Bousmina and R. Muller, *J. Rheol.*, **37**, 663–679 (1993).
7. S. Wu, *Polymer Interface and Adhesion*, Marcel Dekker, New York, 1982.
8. S. Wu, *J. Polym. Sci. C*, **34**, 19 (1971).
9. E. A. Guggenheim, *J. Chem. Phys.*, **13**, 253 (1945).
10. D. Graebing, R. Muller, and J. F. Palierne, *Macromolecules*, **26**, 320–329 (1993).
11. V. Vignaux-Nassiet, A. Allal, and J. P. Montfort, to appear.